Electronic supplementary information for

Thickness-dependent surface reconstructions in non – van der Waals two-dimensional materials

Kai Gao [1], Yan-Jin Chen,[1] Yang Ou,[1], Jin-min Zeng,[1] Chunju Hou[2], Yi Yang,[1]
[1] College of Rare Earths and Faculty of Materials, Metallurgy and Chemistry, Jiangxi University of Science and Technology, Ganzhou, 341000, China
[2] School of Science, Jiangxi University of Science and Technology, Ganzhou, 341000, China

Calculation methods of energetic quantities

The surface energy (E_{surf}^{j}) of Bi_2O_2Se (001) surface (stoichiometric or non-stoichiometric case) was calculated according to the follow equation:[1]

$$E_{surf}^{j} = \frac{1}{2S}\left[E_{slab}^{j} - N_{Bi}\mu_{Bi} - N_{O}\mu_{O} - N_{Se}\mu_{Se}\right] \quad (1)$$

where E_{slab}^{j} (eV) is the total energy of slab *j* and *S* is the area of the surface. N_i is the number of *i* atoms in the slab and μ_i is the chemical potential of element *i* (*i*=Bi, O and Se). For simplicity, relative chemical potential $\Delta\mu_i$ of an element is defined as:

$$\Delta\mu_i = \mu_i - E_i \quad (2)$$

where E_i (eV per atom) is the energy of stable element substance. Assuming that the surface is in equilibrium with the bulk, there is the follow correlation:

$$2\Delta\mu_{Bi} + 2\Delta\mu_{O} + \Delta\mu_{Se} = \Delta H_{bulk} \quad (3)$$

$$\Delta H_{bulk} = E_{bulk} - 2E_{Bi} - 2E_{O} - E_{Se} = -4.913 \text{ eV} \quad (4)$$

where ΔH_{bulk} is the formation energy of Bi_2O_2Se bulk with respect to the element substances and E_{bulk} is the total energy of Bi_2O_2Se bulk. Since we focus on the effect of Se-vacancies (V_{Se}) on the surface stability, there is $N_{Bi} = N_O$ for all surfaces we considered. Substituting eqn (2), (3) and (4) into (1), we obtain the equation of E_{surf}^{j} as a function of $\Delta\mu_{Se}$:

$$E_{surf}^{j} = \lambda^{j} - \frac{1}{2S}\left(N_{Se} - \frac{1}{2}N_{O}\right)\Delta\mu_{Se} \quad (5)$$

where $\lambda^{j} = \frac{1}{2S}\left[E_{slab}^{i} - \frac{1}{2}N_{O}E_{bulk} - \left(N_{Se} - \frac{1}{2}N_{O}\right)E_{Se}\right]$. There are some basic restrictions on the choice of chemical potentials:

$$\Delta\mu_{Bi} < 0\ ;\ \Delta\mu_{O} < 0;\quad \Delta\mu_{Se} < 0 \quad (6)$$

$$2\Delta\mu_{Bi} + 3\Delta\mu_{Se} < \Delta H_{Bi_2Se_3}\ (\Delta H_{Bi_2Se_3} = -1.966\ eV) \quad (7)$$

$$2\Delta\mu_{Bi} + 3\Delta\mu_{O} < \Delta H_{Bi_2O_3}\ (\Delta H_{Bi_2O_3} = -6.171\ eV) \quad (8)$$

$$-2.397\ eV < 2\Delta\mu_{Bi} + 3\Delta\mu_{Se} < -1.966 eV \quad (9)$$

$$-0.799\ eV < \Delta\mu_{Se} < 0\ eV \quad (10)$$

Eqn (6) avoids the formation of element substances. Eqn (7) and (8) preclude the formation of binaries phases Bi_2Se_3 and Bi_2O_3. Combining eqn (3), (7) and (8), we obtain the eqn (9) which gives a restriction to the chemical potential ranges of Se and Bi. Using the eqn (6), we derive the eqn (10) which gives the allowed range for $\Delta\mu_{Se}$. $\Delta H_{Bi_2Se_3}$ and $\Delta H_{Bi_2O_3}$ define the formation energies of Bi_2Se_3 and Bi_2O_3 bulk with respect to the element substances, respectively. Our calculated formation energy of

−6.171 eV for Bi_2O_3 is in good agreement with a previous experimental value of −5.907 eV (0 K) [2] and a theoretical value of −6.531 eV (calculated by PBEsol functional). [3] The calculated value of −1.966 eV for Bi_2Se_3 also agree well with a previously theoretical value of −1.964 eV (calculated by LDA functional).[4]

Cleavage energy (E_{cl}) is the energy cost in cleaving the bulk into two surface parts. For Bi_2O_2X (001) stoichiometric surfaces, the cleavage energy was calculated as follows:

$$E_{\mathrm{cl}} = \frac{1}{2S}\left(E_{\mathrm{slab}}^{\mathrm{unrel}} - NE_{\mathrm{bulk}}\right) \tag{11}$$

where $E_{\mathrm{slab}}^{\mathrm{unrel}}$ and E_{bulk} are the total energies of unrelaxed slab (eV) and the bulk Bi_2O_2X (eV per formula unit), respectively, and N is the number of formula units of Bi_2O_2X in the slab. **The relaxation energy** (E_{rel}) of a slab can be calculated according to the following equation:

$$E_{\mathrm{rel}} = \frac{1}{2S}\left(E_{\mathrm{slab}}^{\mathrm{rel}} - E_{\mathrm{slab}}^{\mathrm{unrel}}\right) \tag{12}$$

where $E_{\mathrm{slab}}^{\mathrm{rel}}$ is the total energy of a relaxed slab. The sum of the cleavage energy and the relaxation energy is the surface energy (E_{surf}) for a stoichiometric surface:

$$E_{\mathrm{surf}} = E_{\mathrm{cl}} + E_{\mathrm{rel}} = \frac{1}{2S}\left(E_{\mathrm{slab}}^{\mathrm{rel}} - NE_{\mathrm{bulk}}\right) \tag{13}$$

For stoichiometric surfaces, the eqn (5) can be simplified to the eqn (13).

Exfoliation energy (E_{ex}) is defined as the energy cost in exfoliating an l-layers ultrathin film from the surfaces. The E_{ex} of 2D Bi_2O_2X (per unit surface area) were calculated by using a rigorous method proposed by Jung et al:[5]

$$E_{\mathrm{ex}} = \frac{1}{S}(E_{\mathrm{l}} - E_{\mathrm{bulk}}) \tag{14}$$

where E_{l} is the total energy of an l-layers ultrathin film. The dimer-, zipper- and uniform-models are considered to make a comparison of their stability and illustrate the thickness-dependence of surface stability. The calculated values are displayed in Fig. 4 and tabulated in Table S2. Note that the formula used in calculating E_{surf} and E_{ex} are similar for the stoichiometric cases with a difference of a factor of 1/2, resulting in that the exfoliation energy of a 2D structure converge to the double of the corresponding surface energy. For the Bi_2O_2S dimer- and uniform-surfaces, the convergence is not as well as other cases, which can be attributed to different structure models used in calculating E_{surf} and E_{ex}, i.e., the middle-layers of the slab models are fixed during structural relaxations for simulating the surfaces, while the slabs for 2D Bi_2O_2X are fully relaxed.

Convergence of the surface energy

We check the convergence of the surface energy of Bi_2O_2Se (001) surface with respect to the thickness of slab. For simplicity, we use the dimer- and zipper-surfaces to test the convergence. Table S1 lists the surface energies for three- to eight-layers slabs. The surface energy of the dimer-surface converges to a value of 0.343 J/m^2 at the thickness of eight-layers. Notably, except for the thinnest slab of three-layer case, there is odd-even oscillation for the surface energy of the zipper-surface. A similar oscillation was also found for the surface energy of Bi_2O_2Se (100) surface.[6] The difference in the

surface energies between the zipper- and dimer-models is 0.02 J/m^2 or 0.04 J/m^2 for five- to eight-layers. Due to limited computing resources, we use relatively thinner slabs of four-layers to simulate the surfaces. Based the four-layers slabs, the difference in the surface energies between the zipper- and dimer-models is about 0.03 J/m^2, which is just located between two limits. Thus, four-layers slabs are utilized to explore the surface properties, unless specifically stated. Using a thick enough slab, we also calculated the surface energy of Bi_2O_2Se (100) surface to be 0.478 J/m^2, which is consistent with a previously reported value of 0.487 J/m^2.[6]

Comparison of PBE and HSE06 methods in calculating electronic structures

It is worth noting that the band gaps of the bulk and the surfaces calculated by PBE functional are underestimated in comparison with the experimental values due to the well-known weakness of semi-local functionals in underestimating the band gaps of semiconductors. In particular, the Bi_2O_2Te bulk was predicted to be metallic, while the Bi_2O_2Te surfaces with 50% V_{Te} were calculated be metallic or semiconducting with a very narrow band gap (around 0.001 eV). We make a comparison of the electronic structures obtained from PBE with those from HSE06+SOC based on a typical small system, i.e., the Bi_2O_2Te zipper-bilayer. Fig. S5 shows the DOS calculated by using HSE06+SOC and PBE. It is seen that the main features of the DOS are overall consistent with each other, except for a larger band width and larger gap provided by HSE06+SOC. It is worth noting that there are no noticeable in-gap states for the Bi_2O_2Te zipper-bilayer with many V_{Te} on the surfaces. This indicates that PBE can provide a reasonable description about the electronic structures of Bi_2O_2X bulk and surfaces.

Surface relaxation effects

Strong relaxation effects of the surfaces can be indicated by the changes of bond lengths and charge states. Taking Bi_2O_2Se as an example, we analyze the bond lengths and the Bader charges of relaxed dimer-surface and make a comparison with the values of the bulk and unrelaxed surface. Fig. S6 shows the bond lengths of Bi-O and Bi-Se located at the surface. It is seen that the bond lengths of Bi-Se in the top surface layer are reduced from a bulk value of 3.322 Å to 2.872 Å and 3.216 Å. Reduced bond lengths at the surfaces indicate stronger interaction strengths of surface ions, implying enhanced stability for this type of surface reconstruction.

We further analyze the Bader charges of ions for the relaxed/unrelaxed surfaces and the bulk. For unrelaxed surface, relative positions of all ions remain the same as those in the bulk and thus bond lengths remain the same. The differences in the Bader charges of ions between the unrelaxed surface and the bulk originate from unsaturated passivation of the surface atoms due to the broken bonds at the surface. For example, the Bader charges of the surface Se are -0.64 e and -0.68 e, whose absolute values are much lower in magnitude than the value of the bulk (-0.96 e). Similarly, in the subsurface Bi layer, the Bi bonded to zero, two and four Se atoms have the Bader charges of 1.25, 1.39 (or 1.41) and 1.53 e, respectively, indicating less charge transfer from Bi to Se for the Bi with more unsaturated bonds. In the subsurface O layer, the absolute values of the Bader charges of O are also lower than the bulk value. However,

the distinction is not so obvious as those of Se and Bi since subsurface O atoms have a coordination environment similar to that in the bulk.

After surface structural relaxation, the charge transfer from cations to anions is enhanced for the surface Se-layer, subsurface Bi-layer, and subsurface O-layer. The relaxation leads to charged states closer to those in the bulk. The most significant change occurs to the bare Bi (bonded to zero Se atoms) whose Bader charge increases about 0.41 e. Therefore, increased charge transfer after the relaxation enhances the interactions between cations and anions, which is consistent with the reduced bond lengths. Enhanced interaction strength lowers the total energy of the surface significantly, which is consistent with considerable relaxation energy.

For the zipper-surface, similarly, the bond lengths are reduced and the charge transfer is enhanced at the surface after relaxation compared with the bulk values **(**Fig. S7**)**. In contrast, the structural relaxation effects are much weaker for the uniform-surfaces. The Bader charges of the surface Se are varied from -0.89 e to -0.93 e after relaxation, while the charges of the subsurface Bi remain almost unchanged (1.62 to 1.63 e). The charge states of the ions in inner layers remain unchanged after relaxation. Weak relaxation effects for the uniform-surfaces are consistent with the low relaxation energies. For Bi_2O_2S and Bi_2O_2Te, the dimer- and zipper-surfaces exhibit similar relaxation effects to those of Bi_2O_2Se, which are evidenced by the changes of bond lengths and charge states at the surfaces during the relaxation (Fig. S8~S11). For instance, the lengths of surface Bi-S bonds are significantly reduced for both dimer- and zipper-surfaces in Bi_2O_2S (see Fig. S8 and S9).

Table S1 surface energy (E_{surf}, J/m^2) of Bi_2O_2Se (001) surface as a function of thickness based on the zipper- or dimer-model.

Layers		3	4	5	6	7	8
E_{surf}	zipper	0.386	0.385	0.371	0.383	0.363	0.383
	dimer	0.355	0.354	0.350	0.344	0.342	0.343

Table S2 Calculated exfoliation energies (E_{ex}) of monolayer (ML), bilayer (BL), trilayer (TL) and quadruple-layer (QL) for Bi_2O_2X. The energetic quantities are in the unit of J/m^2. The lowest E_{ex} value for each 2D Bi_2O_2X is presented as bold.

Case		Bi_2O_2S	Bi_2O_2Se	Bi_2O_2Te
ML	dimer	0.560	0.597	0.527
	zipper	**0.459**	**0.535**	**0.482**
	uniform	0.686	1.186	0.955
BL	dimer	0.662	**0.705**	**0.637**
	zipper	**0.558**	0.766	0.721
	uniform	1.052	1.236	0.996
TL	dimer	**0.623**	**0.678**	**0.617**
	zipper	0.689	0.763	0.727
	uniform	0.990	1.230	0.995
QL	dimer	**0.625**	**0.680**	**0.617**
	zipper	0.692	0.764	0.724
	uniform	1.022	1.228	0.997

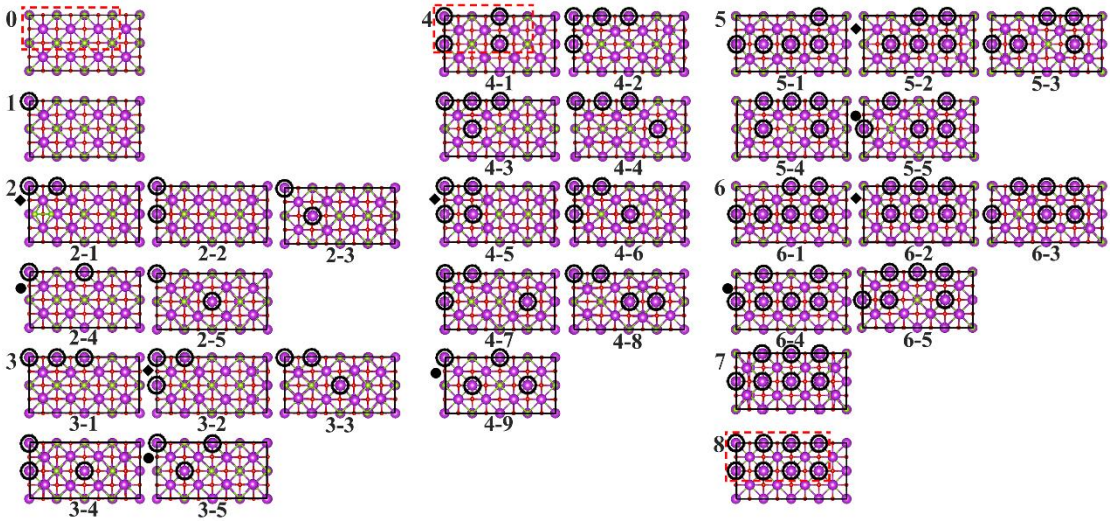

Fig. S1 Top views of all V_{Se} models of Bi_2O_2Se (001) surfaces. The positions of the V_{Se} are marked with circles. For some compositions with several configurations, the most and least sable configurations are marked with diamonds and dots, respectively. Similar structural models are utilized for Bi_2O_2S and Bi_2O_2Te.

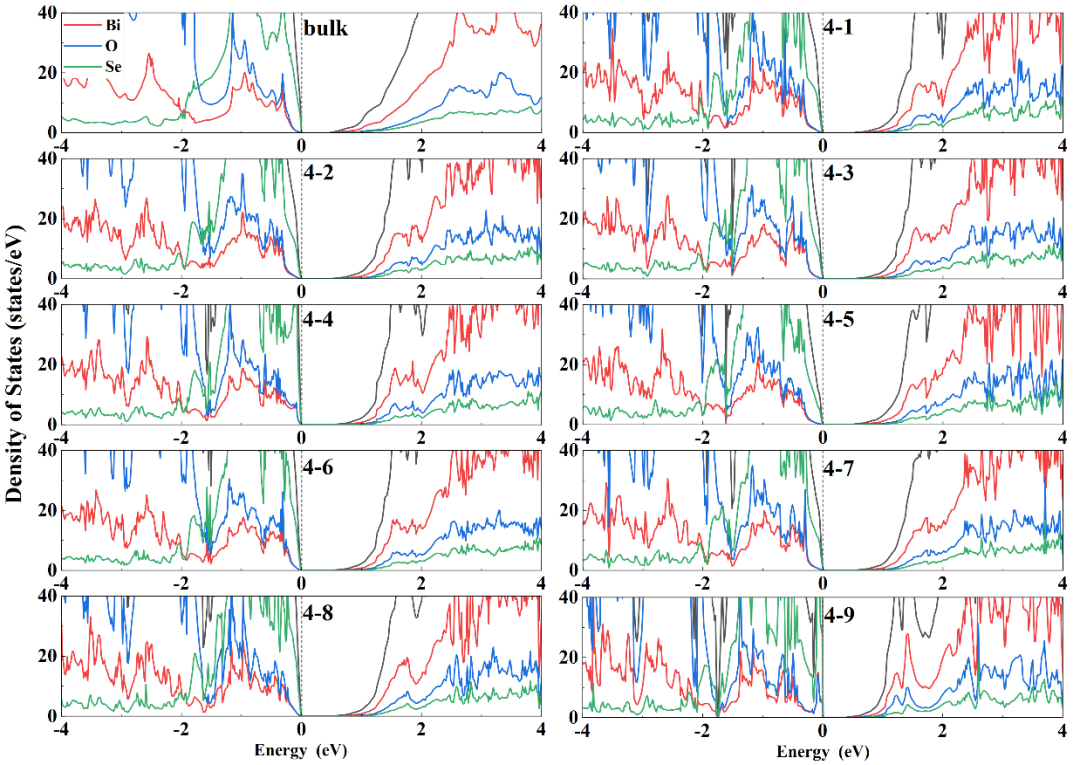

Fig. S2 Total (black lines) and projected (color lines) DOS of the Bi_2O_2Se (001) surfaces for all possible configurations with 50% V_{Se}. The DOS of the bulk is displayed as 16 times larger for a comparison with the surfaces. Zero energy indicates the maximum of the VB.

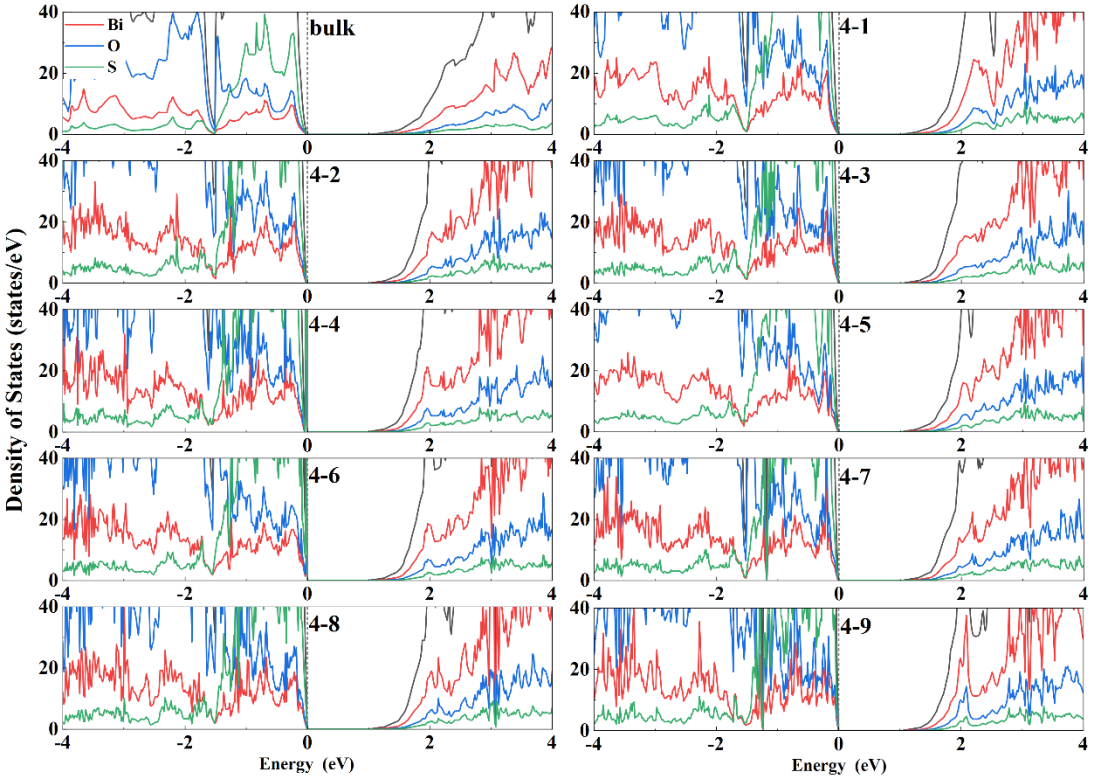

Fig. S3 DOS of the Bi_2O_2S (001) surfaces with 50% V_S.

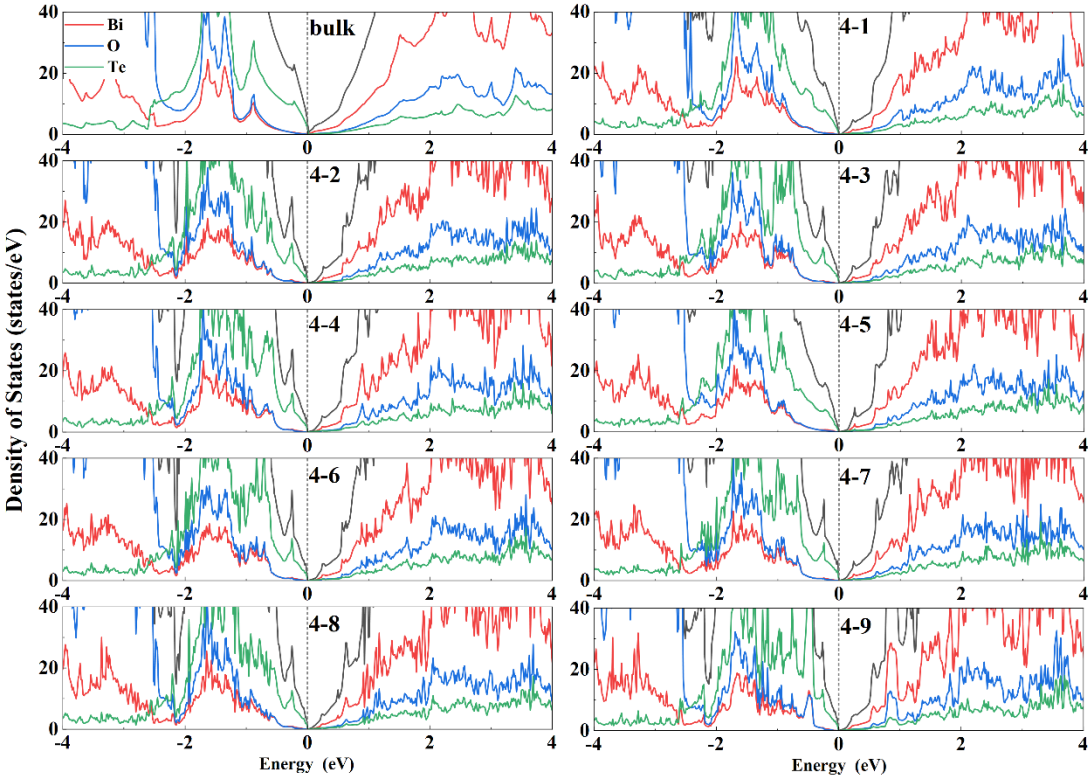

Fig. S4 DOS of the Bi_2O_2Te (001) surfaces with 50% V_{Te}.

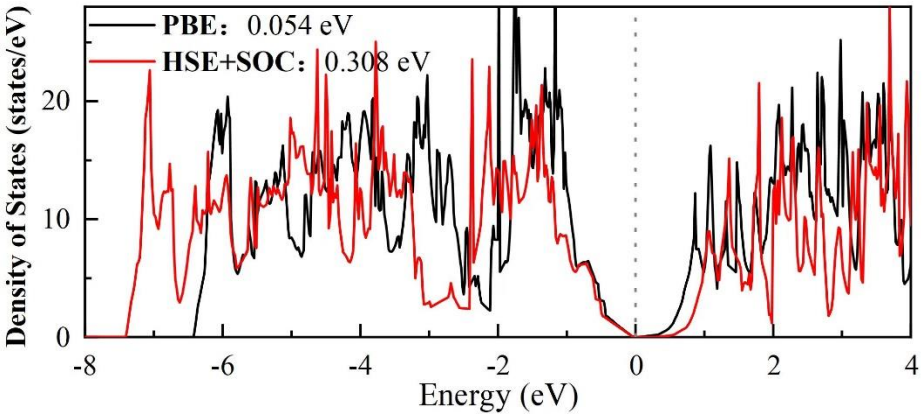

Fig. S5 DOS of the Bi_2O_2Te zipper-bilayer calculated by PBE and HSE06+SOC. The band gaps are shown inset.

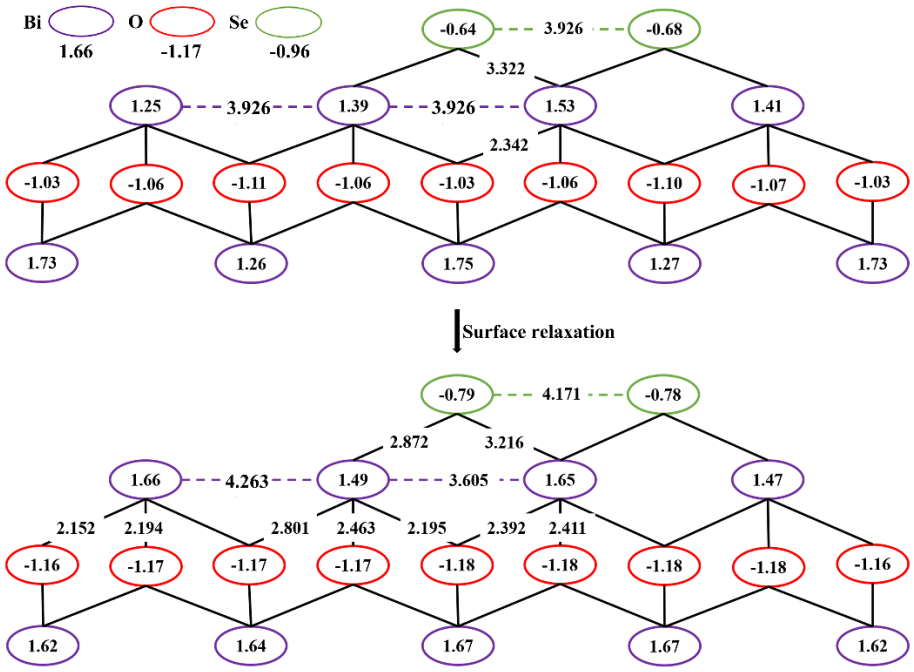

Fig. S6 Bond lengths (numbers on the solid lines between the circles, in unit of Å) and Bader charges of ions (in the circles, in unit of e) in the four atomic layers at the surface for the unrelaxed (top) and relaxed (bottom) **dimer-surfaces of Bi_2O_2Se**. The Bader charges of Bi, O and Se in the bulk are 1.66, -1.17 and -0.96 e, as marked below the circles.

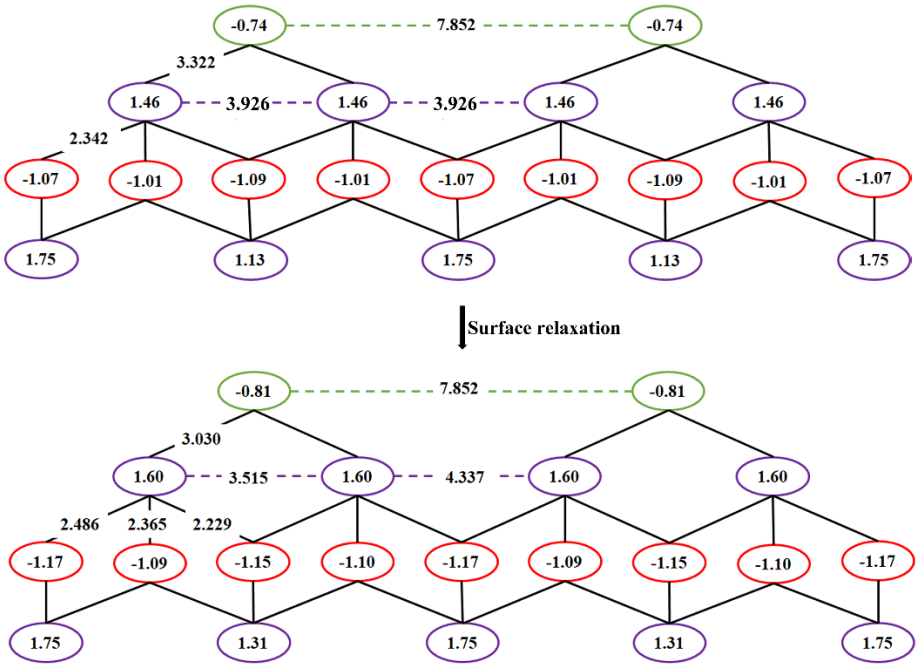

Fig. S7 Bond lengths and Bader charges of ions in the four atomic layers at the surface for the unrelaxed (top) and relaxed (bottom) **zipper-surfaces of Bi_2O_2Se**. The Bader charges of Bi, O and Se in the bulk are 1.66, -1.17 and -0.96 e.

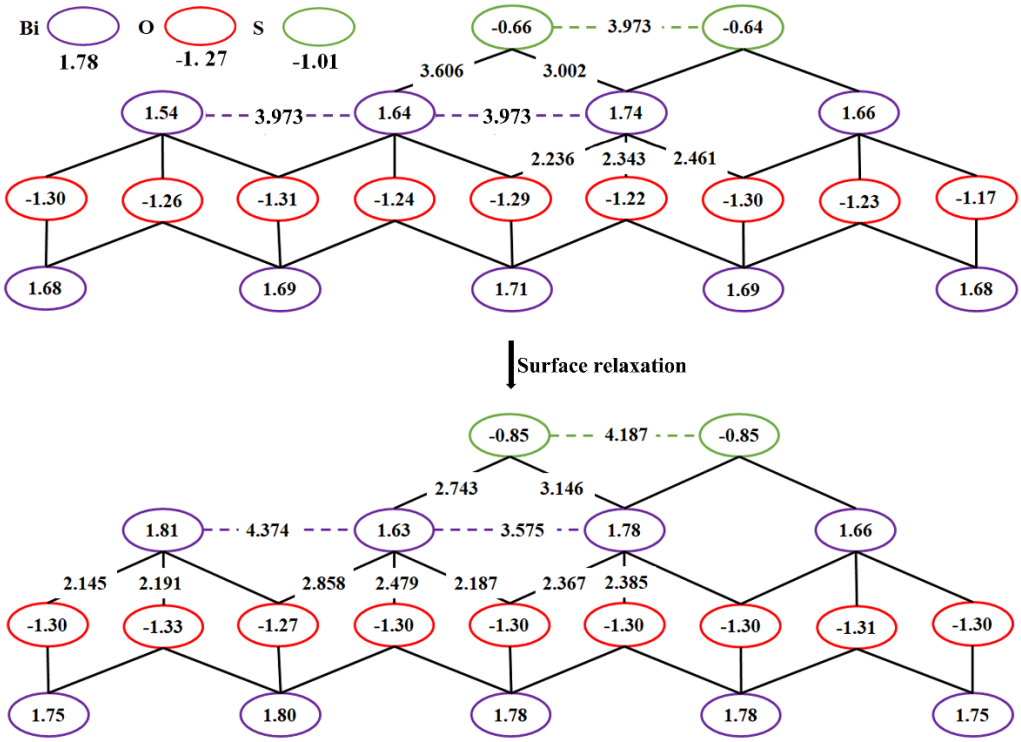

Fig. S8 Bond lengths and Bader charges of ions for the unrelaxed (top) and relaxed (bottom) **dimer-surfaces of Bi_2O_2S**. The Bader charges of Bi, O and S in the bulk are 1.78, -1.27, and -1.01 e.

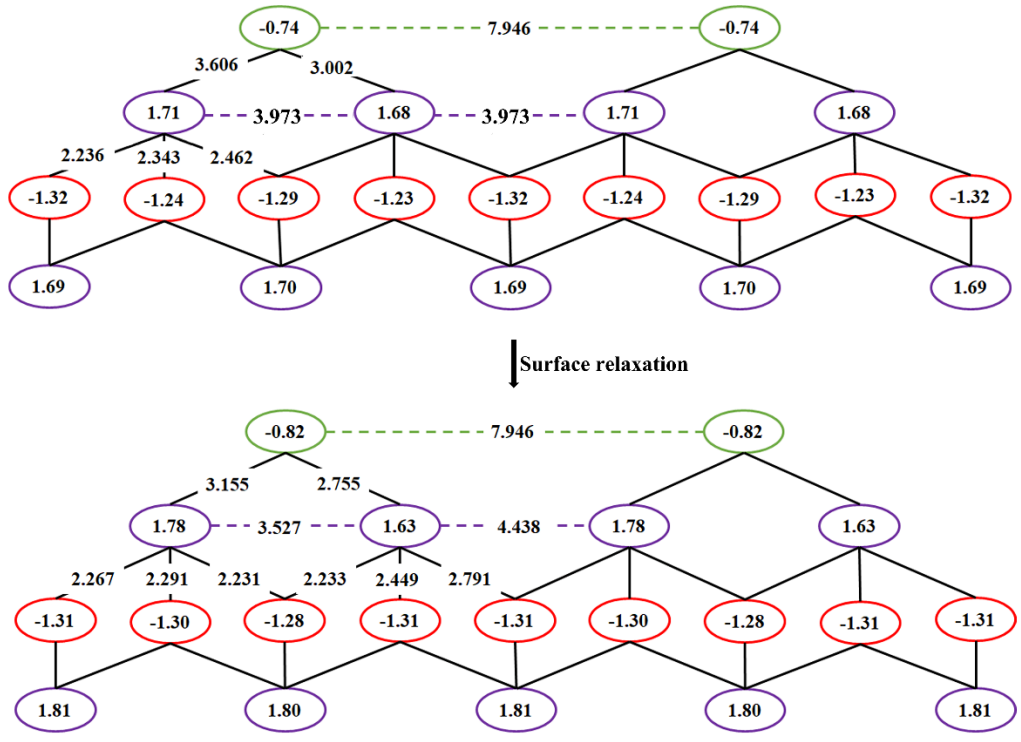

Fig. S9 Bond lengths and Bader charges of ions for the unrelaxed (top) and relaxed (bottom) **zipper-surfaces of Bi_2O_2S**. The Bader charges of Bi, O and S in the bulk are 1.78, -1.27, and -1.01 e.

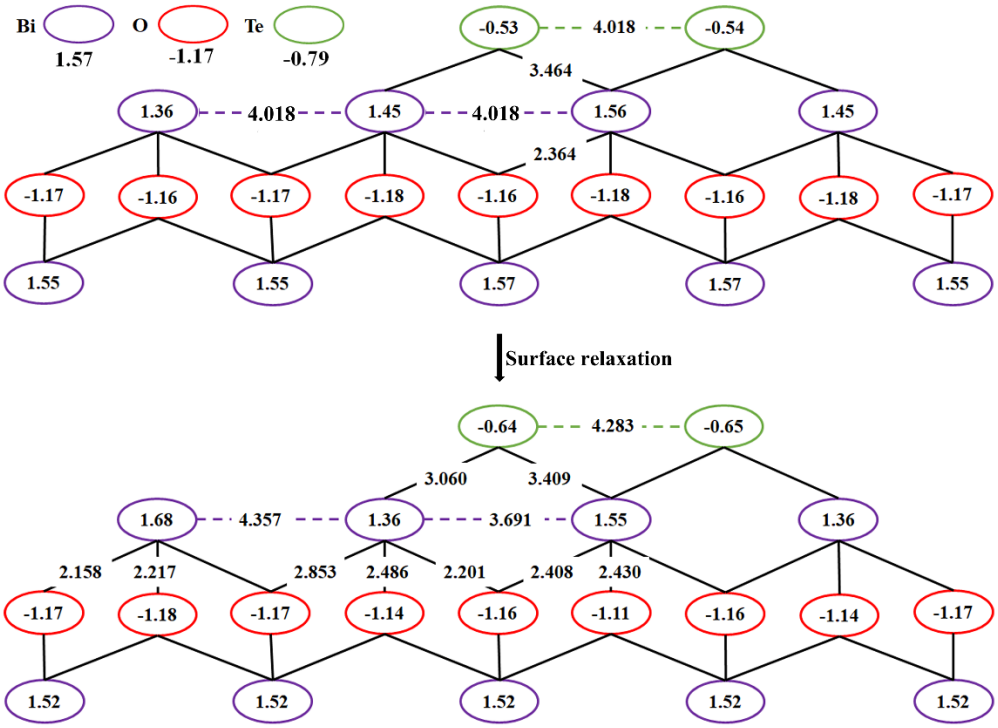

Fig. S10 Bond lengths and Bader charges of ions for the unrelaxed (top) and relaxed (bottom) **dimer-surfaces of Bi_2O_2Te**. The Bader charges of Bi, O and Te in the bulk are 1.57, -1.17 and -0.79 e.

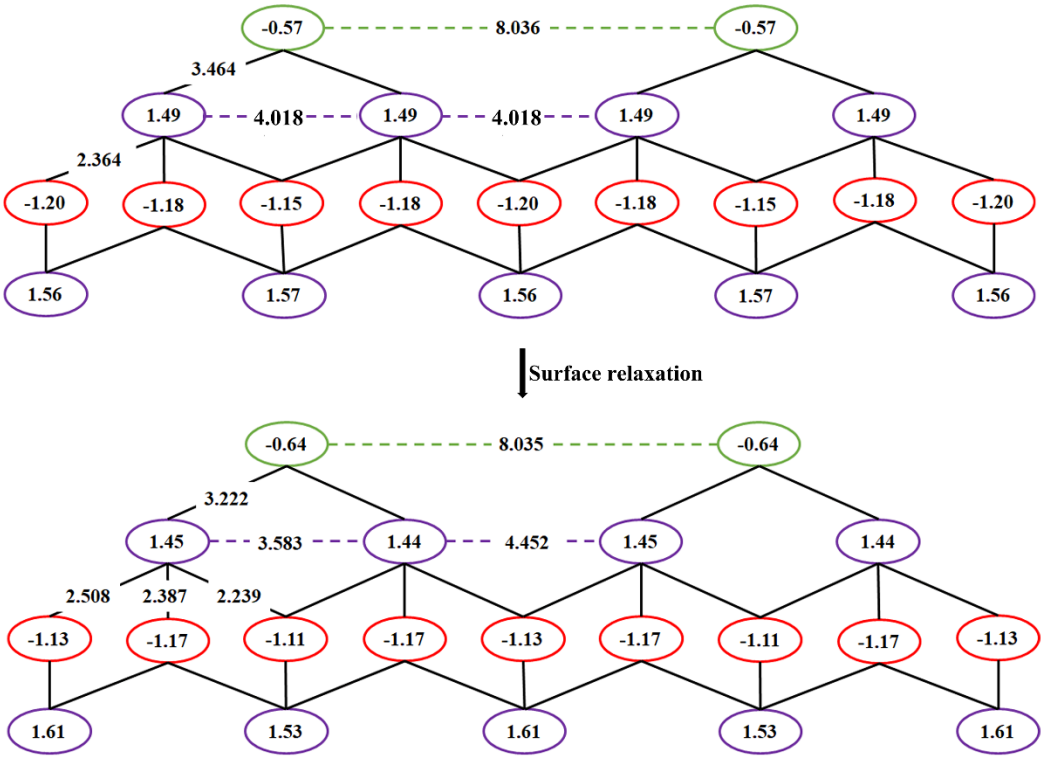

Fig. S11 Bond lengths and Bader charges of ions for the unrelaxed (top) and relaxed (bottom) **zipper-surfaces of Bi_2O_2Te**. The Bader charges of Bi, O and Te in the bulk are 1.57, -1.17 and -0.79 e.

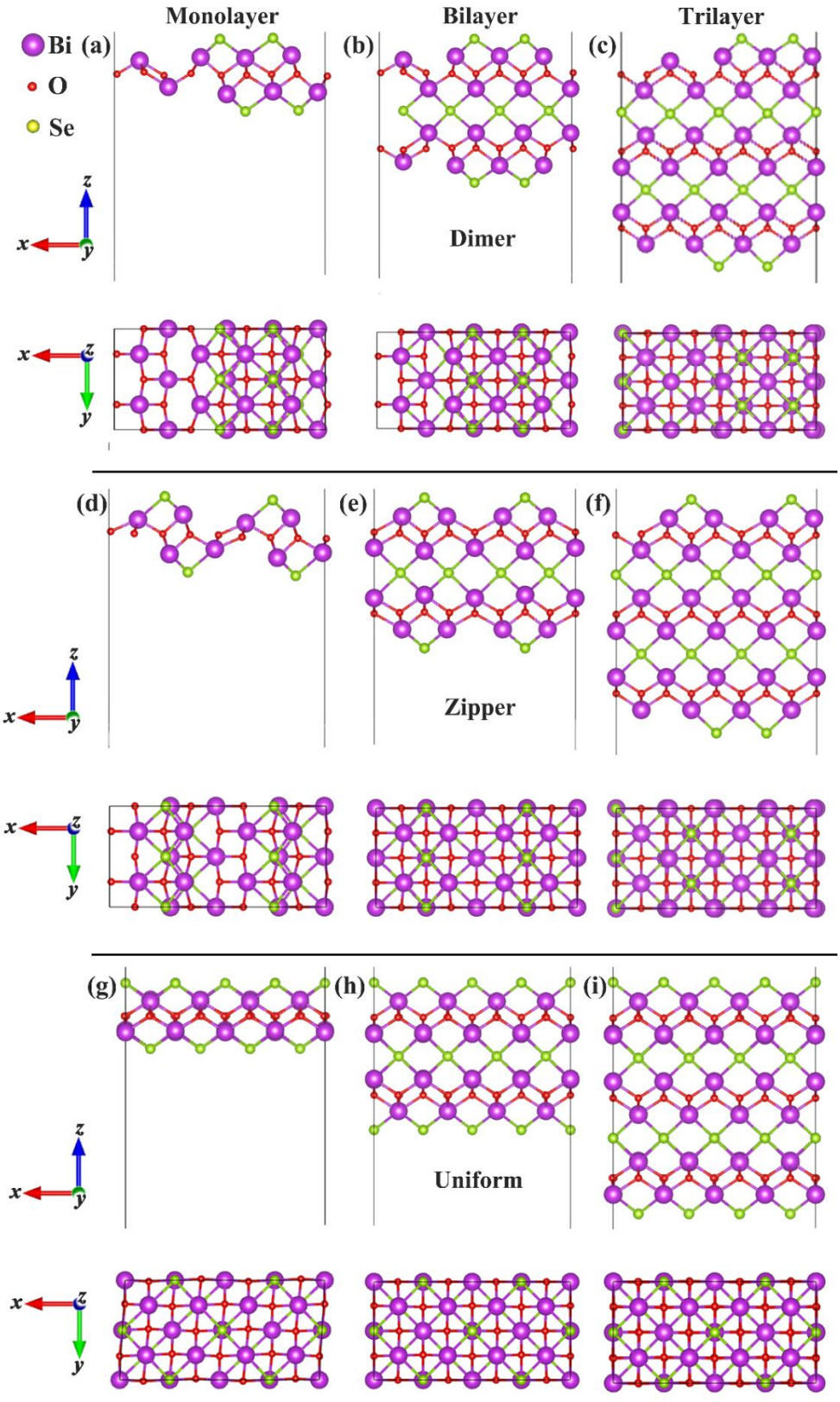

Fig. S12 Structure models of Bi_2O_2Se monolayer (a, d, g), bilayer (b, e, h) and trilayer (e, f, i). Both side and top views are presented. Similar structural models are utilized for Bi_2O_2S and Bi_2O_2Te.

1. G.-X. Qian, R. M. Martin and D. J. Chadi, *Phys. Rev. B*, 1988, **38**, 7649-7663.
2. K. Jacob and A. K. Mansoor, *Thermochim. Acta*, 2016, **630**, 90-96.
3. O. Gomis, F.-J. Manjón, P. Rodríguez-Hernández and A. Muñoz, *J. Phys. Chem. Solids*, 2019, **124**, 111-120.
4. H. Shi, D. Parker, M.-H. Du and D. J. Singh, *Phys. Rev. Appl.*, 2015, **3**, 014004.
5. J. H. Jung, C.-H. Park and J. Ihm, *Nano Lett.*, 2018, **18**, 2759-2765.
6. H. Guo, J. Xiao, J. Qu, D. Legut and Q. Zhang, *J. Phys. Chem. C*, 2019, **123**, 24024-24030.